

# An approximate self-consistent theory of the magnetic field of fluted penumbrae

T. Neukirch<sup>1</sup> and P. C. H. Martens<sup>2</sup>

<sup>1</sup> School of Mathematical and Computational Sciences, University of St. Andrews, St. Andrews, KY16 9SS, Scotland  
email: thomas@dcs.st-and.ac.uk

<sup>2</sup> Space Science Department of ESA at Goddard Space Flight Center, Code 682.3, NASA/GSFC, Greenbelt, MD 20771  
email: pmartens@esa.nascom.nasa.gov

Received date; accepted date

**Abstract.** A self-consistent mathematical description of the magnetic field of fluted sunspot penumbrae is presented. This description is based on an expansion of the nonlinear force-free magnetohydrostatic equations written in cylindrical coordinates. The lowest order solutions are mathematically equivalent to laminated force-free equilibria in Cartesian geometry. The lowest order solutions have no toroidal component of the magnetic field and the magnetic pressure does not vary with azimuth but the solutions allow arbitrary variations of the magnetic field components with azimuth. Explicit solutions are presented which have a realistic radial profile of the magnetic field strength and reproduce the basic features of the observations.

**Key words:** Sunspots – Sun: magnetic fields – MHD – Methods: analytical

## 1. Introduction

Sunspot penumbrae show structures in the form of alternating dark and bright fibrils extending in the radial direction across the penumbra. Observations by Beckers & Schröter (1969) have already suggested that the magnetic field inside the dark filaments might be close to horizontal whereas the field in the bright filaments is less inclined with respect to the vertical. This magnetic field structure has implications for the Evershed flow which was also suggested to be associated mainly with the dark filaments. The association of the Evershed flow with the dark penumbral fibrils has recently been confirmed by Shine et al. (1994) and Rimmele (1994, 1995b). In these observations, it was also found that the Evershed effect is a quasi-periodic time-dependent phenomenon which extends beyond the penumbral boundary (Rimmele 1995b). Furthermore, there is evidence (Rimmele 1995a) that the Evershed flow occurs in thin channels which are elevated above the continuum height for most parts of the penumbra. Very recently, Westendorp-Plaza et al. (1997) have actually for the first time identified the regions of return flux for the field lines carrying the Evershed flow. Their

observations support the view that the Evershed flow is carried by low-lying field lines.

The suggested spatial variation of the inclination angle of the magnetic field with azimuth was also found by Lites et al. (1990) and Degenhardt & Wiehr (1991). Recently, very high resolution observations with the Lockheed tunable filtergraph on the Swedish Solar Observatory in La Palma (Title et al. 1993) showed that the magnetic field of a sunspot penumbra indeed varies between nearly horizontal in the dark penumbral filaments and much less inclined in the bright filaments. Similar results were obtained by Rimmele (1995a) and StachfieldII et al. (1997). The observations of Title et al. (1993) show that the mean inclination of the magnetic field increases from 40°-50° to 70°-75° across the penumbra and that there is a rapid azimuthal variation of the inclination angle of about 18°. Little or no variation of the total field strength with azimuth is found by Title et al. (1993) and Rimmele (1995a) (see, however, the discussion in StachfieldII et al. (1997)). On the basis of these observations, Title et al. (1993) proposed a tentative model for the magnetic field structure, which resembles that of laminated force-free fields (Low 1988a, 1988b). Since these fields only exist for Cartesian and spherical geometry, the model of Title et al. (1993) could so far not be backed up by a self-consistent calculation.

In a recent paper, Martens et al. (1996) presented a linear force-free model for a fluted sunspot. The model is able to explain some of the properties of fluted sunspots. Due to the high azimuthal wave number of the fluted force-free component, the scale height of this component is very small and the flutedness is confined to the chromosphere in this model. Furthermore, the magnetic loops corresponding to the dark filaments are very short in this model and the filaments do consist of a series of loops. This implies that the Evershed flow would have to consist of a phase-coordinated flow along many short loops. There is no explanation how this could be achieved. Therefore there is a clear need for improved models.

The fundamental problem posed by the observations is that a genuinely three-dimensional solution of the magnetohydrostatic equations is necessary. Though there has been some progress concerning analytical solutions in three dimensions re-

cently (e.g. Neukirch 1995, 1997), these solutions do either not apply to the problem or they suffer from the same deficiencies as the linear force-free solutions. A different approach is therefore necessary.

In the present paper we present a method which allows us to find a self-consistent version of the model originally put forward by Title et al. (1993). The method is based on an asymptotic expansion of the three-dimensional force-free equations. The lowest order of this expansion has solutions which are formally equivalent to laminated force-free fields and a large number of different solutions can be found. These solutions can be used to model the magnetic field of the penumbra of a fluted sunspot.

In the following, we first briefly review the theory of laminated force-free fields and then present the expansion procedure. A specific solution which is useful as a model for a fluted penumbral magnetic field is presented and its properties are discussed especially in connection with a theoretical explanation of the Evershed flow.

## 2. Basic Theory

### 2.1. Non-existence of laminated force-free fields in cylindrical coordinates

We assume that the magnetic field of the sunspot penumbra is force-free and therefore obeys the equations

$$\begin{aligned} \mathbf{j} \times \mathbf{B} &= 0, & (1) \\ \nabla \times \mathbf{B} &= \mu_0 \mathbf{j}, & (2) \\ \nabla \cdot \mathbf{B} &= 0. & (3) \end{aligned}$$

From Eq. (1) we conclude that

$$\begin{aligned} \nabla \times \mathbf{B} &= \alpha \mathbf{B}, & (4) \\ \mathbf{B} \cdot \nabla \alpha &= 0, & (5) \end{aligned}$$

where we have absorbed  $\mu_0$  into  $\alpha$ .

The observations (Degenhardt & Wiehr 1991; Title et al. 1993; Rimmele 1995a) show that simple sunspots may have a fluted penumbra with rapid variations of the inclination of the magnetic field with azimuth ( $\phi$ ), however with almost constant magnetic pressure at constant radius. Also the electric currents seem to flow mostly in the meridional planes ( $\phi = \text{constant}$ ). The appropriate model to describe such a magnetic field would be given by laminated non-linear force-free fields (Low 1988a, 1988b). However, these fields do only exist in Cartesian and spherical coordinates; in cylindrical coordinates appropriate for the description of sunspots such fields do not exist. This can be most easily seen as follows. The basic assumption is

$$\mathbf{B} = (B_r, 0, B_z), \quad (6)$$

$$\alpha = \alpha(\phi). \quad (7)$$

Then Eq. (5) is automatically fulfilled. If we take the curl of Eq. (2) and multiply the result by  $\mathbf{e}_\phi$  we get

$$\mathbf{e}_\phi \cdot \nabla \times (\nabla \times \mathbf{B}) = \alpha^2 B_\phi + \frac{1}{r} \frac{d\alpha}{d\phi} \mathbf{e}_\phi \cdot \mathbf{e}_\phi \times \mathbf{B} = 0. \quad (8)$$

On the other hand

$$\mathbf{e}_\phi \cdot \nabla \times (\nabla \times \mathbf{B}) = -\nabla^2 B_\phi - \frac{2}{r} \frac{\partial B_r}{\partial \phi} + \frac{2B_\phi}{r^2} = -\frac{2}{r} \frac{\partial B_r}{\partial \phi}. \quad (9)$$

It follows that  $B_r$  may not depend on  $\phi$  which precludes flutedness for force-free fields in cylindrical coordinates. This means that only rotationally symmetric equilibria of this type are possible and therefore it is impossible to find an exact force-free solution appropriate for fluted sunspots.

### 2.2. Asymptotic expansion method

However, if we are mainly interested in the penumbral structure, we could try to find an approximate solution with the desired properties, based on laminated equilibria. We start by writing Eqs. (4) and (5) together with Eq. (3) in cylindrical coordinates:

$$\frac{1}{r} \frac{\partial B_z}{\partial \phi} - \frac{\partial B_\phi}{\partial z} = \alpha B_r, \quad (10)$$

$$\frac{\partial B_r}{\partial z} - \frac{\partial B_z}{\partial r} = \alpha B_\phi, \quad (11)$$

$$\frac{1}{r} \frac{\partial}{\partial r} \left( \frac{1}{r} B_\phi \right) - \frac{1}{r} \frac{\partial B_r}{\partial \phi} = \alpha B_z, \quad (12)$$

$$B_r \frac{\partial \alpha}{\partial r} + B_\phi \frac{1}{r} \frac{\partial \alpha}{\partial \phi} + B_z \frac{\partial \alpha}{\partial z} = 0, \quad (13)$$

$$\frac{1}{r} \frac{\partial}{\partial r} (r B_r) + \frac{1}{r} \frac{\partial B_\phi}{\partial \phi} + \frac{\partial B_z}{\partial z} = 0. \quad (14)$$

We now introduce a new radial coordinate

$$\varpi := \frac{r^2 - a^2}{2a}, \quad (15)$$

where  $a$  is a yet unspecified radius located somewhere inside the penumbra (actually  $a$  could be treated as a free parameter which can be used later to minimise the residual force resulting from the approximation). If the radial extent of the penumbra is  $2R_p$ , we now expand the equations above in the parameter

$$\epsilon = R_p/a, \quad (16)$$

which we assume to be smaller than one (this is a kind of large-aspect-ratio expansion with  $1/\epsilon$  being the aspect ratio). This type of expansion procedure together with the coordinate transformation Eq. (15) has been introduced by Kiessling (1995) in the framework of toroidally confined plasma equilibria.

With  $r = a\sqrt{1 + 2\epsilon\varpi/R_p}$  we get

$$\frac{1}{a\sqrt{1 + 2\epsilon\varpi/R_p}} \frac{\partial B_z}{\partial \phi} = \alpha B_r, \quad (17)$$

$$\frac{\partial B_r}{\partial z} - \sqrt{1 + 2\epsilon\varpi/R_p} \frac{\partial B_z}{\partial \varpi} = \alpha B_\phi, \quad (18)$$

$$\frac{\partial}{\partial \varpi} \left( \sqrt{1 + 2\epsilon\varpi/R_p} B_\phi \right) - \frac{1}{a\sqrt{1 + 2\epsilon\varpi/R_p}} \frac{\partial B_r}{\partial \phi} = \alpha B_z, \quad (19)$$

$$\sqrt{1 + 2\epsilon\varpi/R_p} B_r \frac{\partial\alpha}{\partial\varpi} + B_\phi \frac{1}{a\sqrt{1 + 2\epsilon\varpi/R_p}} \frac{\partial\alpha}{\partial\phi} + B_z \frac{\partial\alpha}{\partial z} = 0, \quad (20)$$

$$\frac{\partial}{\partial\varpi} \left( \sqrt{1 + 2\epsilon\varpi/R_p} B_r \right) + \frac{1}{a\sqrt{1 + 2\epsilon\varpi/R_p}} \frac{\partial B_\phi}{\partial\phi} + \frac{\partial B_z}{\partial z} = 0, \quad (21)$$

We now introduce the following expansion scheme in  $\epsilon$

$$B_r = \sum_{n=0}^{n=\infty} \epsilon^n B_r^{(n)}(\varpi, \phi, z), \quad (22)$$

$$B_\phi = \sum_{n=1}^{n=\infty} \epsilon^n B_\phi^{(n)}(\varpi, \phi, z), \quad (23)$$

$$B_z = \sum_{n=0}^{n=\infty} \epsilon^n B_z^{(n)}(\varpi, \phi, z), \quad (24)$$

$$\alpha = \sum_{n=0}^{n=\infty} \epsilon^n \alpha^{(n)}(\varpi, \phi, z). \quad (25)$$

Note that  $B_\phi$  is of order  $\epsilon$  whereas all other quantities are of order  $\epsilon^0 = 1$ . To lowest order in  $\epsilon$  we get:

$$\frac{1}{a} \frac{\partial B_z^{(0)}}{\partial\phi} = \alpha^{(0)} B_r^{(0)}, \quad (26)$$

$$\frac{\partial B_r^{(0)}}{\partial z} - \frac{\partial B_z^{(0)}}{\partial\varpi} = 0, \quad (27)$$

$$-\frac{1}{a} \frac{\partial B_r^{(0)}}{\partial\phi} = \alpha^{(0)} B_z^{(0)}, \quad (28)$$

$$B_r^{(0)} \frac{\partial\alpha^{(0)}}{\partial\varpi} + B_z^{(0)} \frac{\partial\alpha^{(0)}}{\partial z} = 0, \quad (29)$$

$$\frac{\partial B_r^{(0)}}{\partial\varpi} + \frac{\partial B_z^{(0)}}{\partial z} = 0. \quad (30)$$

Eqs. (26) - (30) are completely equivalent to the equations for laminated force-free fields in Cartesian geometry (Low 1988a) with the replacements  $x := \varpi$  and  $y := \phi$ .

Multiplying Eq. (26) by  $B_z^{(0)}$  and Eq. (28) by  $-B_r^{(0)}$  and adding the two equations, we get:

$$\frac{\partial}{\partial\phi} \left( B_r^{(0)2} + B_z^{(0)2} \right) = 0. \quad (31)$$

Eq. (29) can be solved by

$$\alpha^{(0)} = \alpha^{(0)}(\phi). \quad (32)$$

Eq. (30) is solved by introducing a flux function  $A(\varpi, \phi, z)$ :

$$\mathbf{B}^{(0)} = \left( -\frac{\partial A}{\partial z}, 0, \frac{\partial A}{\partial\varpi} \right). \quad (33)$$

Inserting Eq. (33) into Eq. (27) we obtain

$$\frac{\partial^2 A}{\partial\varpi^2} + \frac{\partial^2 A}{\partial z^2} = 0. \quad (34)$$

Eqs. (34) and (31) allow solutions of the form (Low 1988a)

$$A(\varpi, \phi, z) = \text{Re} \left( G(\xi) \exp[i\gamma(\phi)] \right), \quad (35)$$

where  $\xi = \varpi + iz$ . So in this approximation we have a field without a  $B_\phi$  component that is potential in the  $\varpi$ - $z$ -plane with an arbitrary modulation in the  $\phi$ -direction.

### 3. Modeling the penumbra of a fluted sunspot

#### 3.1. The Beckers-Schröter profile

The solution (35) at first sight leaves a large degree of freedom to model fluted penumbrae. However, if one wants to calculate fields which reproduce the basic features of the observations the solution class is considerably restricted. We will illustrate this by considering a specific example.

We assume that the basic data we have are the absolute value of the magnetic field ( $B(r)$ ) and the inclination angle  $\delta(r, \phi, 0)$  of the magnetic field with the vertical at the level  $z = 0$ . Within the framework of the theory developed so far, we can only represent spots which have little or no variation of field strength with azimuth. For reasons of mathematical convenience, we assume that

$$B(r) = \frac{B_0}{1 + (r/L)^2}. \quad (36)$$

This is the radial dependence of the field strength deduced by Beckers & Schröter (1969) from their observations. Other radial profiles like that of the Schatzman field (Schatzman 1965) could also be dealt with, but the Beckers-Schröter profile has the advantage of greater mathematical simplicity.

From Eq. (35) the magnetic field is given by

$$B_r = \text{Im} \left( \frac{dG}{d\xi} \exp[i\gamma(\phi)] \right), \quad (37)$$

$$B_z = \text{Re} \left( \frac{dG}{d\xi} \exp[i\gamma(\phi)] \right). \quad (38)$$

The field amplitude is the given by

$$B = \left| \frac{dG}{d\xi} \right|. \quad (39)$$

With the coordinate transformation (15) we rewrite the Beckers-Schröter profile (36) as

$$B(\varpi) = \frac{B_0}{1 + \frac{2a\varpi + a^2}{L^2}}. \quad (40)$$

Modulo a phase factor this profile corresponds to the absolute value of the complex function

$$F_{BS} := \frac{dG}{d\xi} = \frac{B_0}{\frac{2a}{L^2}\xi + 1 + \frac{a^2}{L^2}} \quad (41)$$

on the real axis ( $z = 0$ ). The most general complex function  $\psi(\xi)$  with the same absolute value on the real axis can be written as

$$\psi(\xi) = F_{BS}(\xi) \cdot Q(\xi), \quad (42)$$

with

$$|Q(\xi)| = 1 \quad (43)$$

on the real axis ( $z = 0$ ). As we will see below the inclusion of an appropriate function  $Q$  is indispensable for a proper representation of the penumbral magnetic field. A simple example of such a function  $Q$  is given by

$$Q(\xi) = \exp(iq\xi), \quad (44)$$

with  $q$  a real number. This example also illustrates that it is most convenient to write  $Q(\xi)$  in the form

$$Q(\xi) = \exp(if(\xi)). \quad (45)$$

The magnetic field components are the given by the expressions

$$B_r = \frac{B_0 L^2}{2a} \frac{\exp(-\text{Im}(f))}{\left(\frac{L^2 + a^2}{2a} + \varpi\right)^2 + z^2} \left[ \left(\varpi + \frac{L^2 + a^2}{2a}\right) \sin(\gamma(\phi) + \text{Re}(f)) - z \cos(\gamma(\phi) + \text{Re}(f)) \right], \quad (46)$$

$$B_z = \frac{B_0 L^2}{2a} \frac{\exp(-\text{Im}(f))}{\left(\frac{L^2 + a^2}{2a} + \varpi\right)^2 + z^2} \left[ \left(\varpi + \frac{L^2 + a^2}{2a}\right) \cos(\gamma(\phi) + \text{Re}(f)) + z \sin(\gamma(\phi) + \text{Re}(f)) \right]. \quad (47)$$

Another important piece of information given by the observations is the inclination angle  $\delta$  of the magnetic field vector, i.e. the angle between the magnetic field vector and the vertical direction. For the magnetic field with the components given by Eqs. (46) and (47), the inclination angle is given by the equation

$$\delta(r, \phi, z) = \gamma(\phi) + \text{Re}(f) - \arctan\left(\frac{z}{\varpi + \frac{L^2 + a^2}{2a}}\right), \quad (48)$$

where the last term is the phase of  $F_{BS}$ . We remark that with the present theory, we can only represent fields that have an inclination angle which is additive in the dependence on the azimuth  $\phi$  and the radial coordinate  $\varpi$  for  $z = 0$ . Therefore, we can write the inclination as

$$\delta(\varpi, \phi, z) = \delta_{av}(\varpi, z) + \delta_{mod}(\phi), \quad (49)$$

with the identities

$$\delta_{av}(\varpi, z) = \text{Re}(f) - \arctan\left(\frac{z}{\varpi + \frac{L^2 + a^2}{2a}}\right), \quad (50)$$

$$\delta_{mod}(\phi) = \gamma(\phi). \quad (51)$$

The task now is to find a complex function  $f(\xi)$  which has the property  $\text{Im}(f) = 0$  for  $z = 0$  and which represents the radial variation of the average inclination for  $z = 0$ . At first sight this might seem easy because we have already presented such a function above ( $f(\xi) = q\xi$ ). A closer inspection of the inclination angle and the magnetic field components for values of  $z \neq 0$  reveals, however, that a naive choice of  $f$  will cause problems. For  $z = 0$  the phase of  $F_{BS}$  vanishes, but for  $z \neq 0$  it contributes to the inclination angle. Actually for  $z \rightarrow \infty$  this contribution tends to  $-\pi/2$ . Since the average inclination angle should be positive for  $z = 0$  this implies that the radial magnetic field component will change its sign as  $z$  increases unless  $\text{Re}(f)$  also increases with  $z$  sufficiently fast. In other words, the field lines would bend backwards toward the sunspot center at a finite height  $z$ . This is of course not an acceptable solution. The real part of the linear function  $f(\xi) = q\xi$  for example does not increase with  $z$  and therefore the linear function is not a viable choice.

On the other hand, if  $\text{Re}(f)$  increases without bound for  $z \rightarrow \infty$  the sign of both  $B_z$  and  $B_r$  will change an infinite number of times as the argument of sine, respectively cosine tends to infinity. This as well is not an acceptable solution. We therefore have to find a function  $f(\xi)$  which has a real part that tends to a constant as  $z$  goes to infinity and fulfills all the conditions mentioned previously.

A function which fulfills all these conditions is

$$f(\xi) = q \frac{\xi - L_a}{\xi - L_b} \quad (52)$$

where  $q$ ,  $L_a$  and  $L_b$  are real numbers. The real and imaginary parts of this function are

$$\text{Re}(f) = q \frac{(\varpi - L_a)(\varpi - L_b) + z^2}{(\varpi - L_b)^2 + z^2}, \quad (53)$$

$$\text{Im}(f) = q \frac{(L_a - L_b)z}{(\varpi - L_b)^2 + z^2}. \quad (54)$$

For  $z = 0$  the imaginary part vanishes as required and for  $\varpi$  fixed and  $z \rightarrow \infty$  the real part has the limit  $q$ . Other functions may fulfill these requirements as well, but this form of  $f$  has the advantage of being relatively simple. Of course, if the radial variation of the inclination angle would be given by observations, then the observations would prescribe the real part of  $f$  for  $z = 0$ . Here, however, we are merely interested to illustrate the method developed and therefore choose a simple form of  $f$ . Actually, once one has found one  $f$  with the desired properties, it is possible to add any other complex function  $\bar{f}$  which is bounded for  $z \rightarrow \infty$  and  $\varpi$  fixed. An example of such a function is the linear function  $\bar{f} = \bar{q}\xi$ . This means that even with the restrictions discussed above one still has considerable freedom to model the variation of the average inclination angle with radius across the penumbra.

### 3.2. An example

In the present paper we restrict our treatment to the function  $f$  given in Eq. (52). We treat the parameter  $q$  as a free parameter

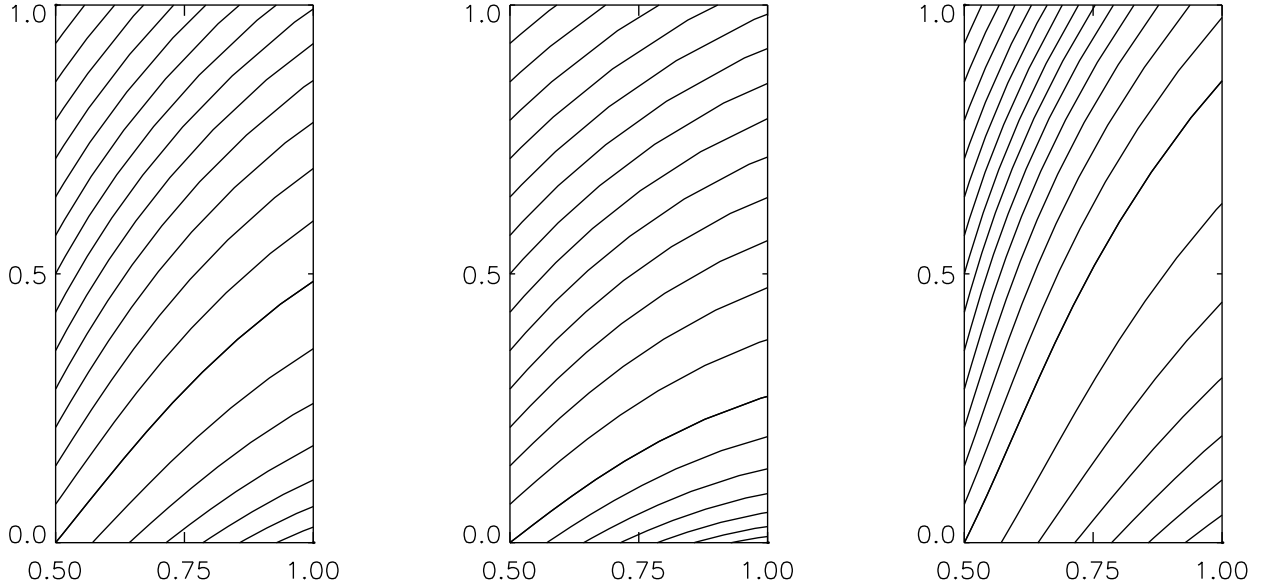


**Fig. 1.** Field line plots in the planes  $\phi = 0$  corresponding to average inclination (left),  $\phi = \pi/4m$  corresponding to maximum inclination (middle) and  $\phi = 3\pi/4m$  corresponding to minimum inclination (right). The field lines plotted cross the lower or left boundaries at the same location in all three plots to facilitate the comparison. Therefore the distance between field lines does not necessarily reflect the strength of the magnetic field.

**Table 1.** Parameter values used in the example shown in Figs. 1, 2 and 3

Parameter	Meaning	Value
$r_o$	outer penumbral radius	1.0
$r_i$	inner penumbral radius	0.5
$a$	origin of transformed radial coordinate	0.8
$q$	amplitude of argument of phase factor	$7\pi/9$
$\delta_{av,i}$	average inclination at inner boundary	$50^\circ$
$\delta_{av,o}$	average inclination at outer boundary	$70^\circ$
$L_a$	parameter of function $f$	-0.562
$L_b$	parameter of function $f$	-1.349
$\bar{\delta}_{mod}$	amplitude of variation	$18^\circ$
$m$	azimuthal wave number	66
$B_i$	field strength at inner boundary	1500 G
$B_o$	field strength at outer boundary	1000 G
$B_0$	amplitude of Beckers-Schröter profile	1.8
$L$	length scale of Beckers-Schröter profile	1.118

which we choose such that we get a satisfying field line shape. The parameters  $L_a$  and  $L_b$  are determined by imposing the (average) inclination angles at the inner and outer boundary of the penumbra. This leads to two simple linear equations for  $L_a$  and  $L_b$ .

For the example we choose the outer boundary of the penumbra to be normalized ( $r_o = 1.0$ ) and the inner boundary of the penumbra to be located at  $r_i = 0.5$ . The origin of the transformed coordinate system is chosen as  $a = 0.8$  locating it approximately halfway between the inner and outer boundary

of the penumbra. The (average) inclination angles at the inner and outer boundary are chosen as  $\delta_{av,i} = 50^\circ$  and  $\delta_{av,o} = 70^\circ$ . In this example we have chosen  $q = 7\pi/9$ . The value of  $q$  influences the inclination of the field lines for  $z \neq 0$ . Higher values of  $q$  give a larger inclination for large  $z$  and vice versa. The resulting values for  $L_a$  and  $L_b$  are listed together with the other parameter values in Table 1.

For the modulation of the inclination angle with  $\phi$ , we choose a simple harmonic function

$$\delta_{mod}(\phi) = \gamma(\phi) = \bar{\delta}_{mod} \sin(m\phi) \quad (55)$$

The parameter  $\bar{\delta}_{mod}$  is the amplitude of the inclination variation which we choose to be  $18^\circ$  and  $m$  is the azimuthal wavenumber of the variation which we choose to be 66 in accordance with Martens et al. (1996). Of course, any other modulation with azimuth would be possible as well as long as it is periodic with period  $2\pi$ .

The last two parameters to determine are those of the magnetic field strength, namely  $B_0$  and  $L$ . These parameters will be determined by the measured values of the magnetic field strength at the inner and outer boundary ( $B_i$  and  $B_o$ ). In the present example we have taken  $B_i = 1500$  G and  $B_o = 1000$  G. Again, from the two conditions on the inner and outer penumbral boundary, we get two equations for the parameters  $B_0$  and  $L$ , which can be easily solved. For the field strengths used we also give the values of  $B_0$  and  $L$  in Table 1. The results are shown in Figs. 1 and 2. In Fig. 1 we show field line plots of the field lines in the planes  $\phi = 0$ ,  $\phi = \pi/4m$  and  $\phi = 3\pi/4m$  corresponding to average, maximum and minimum inclination.

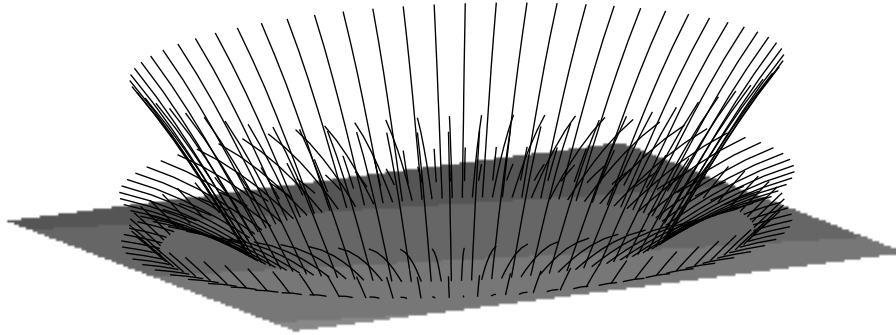


**Fig. 2.** Three-dimensional plot of sets of field lines originating close to the inner and outer penumbral boundary. The flutedness of the field is obvious. The azimuthal wave number is  $m = 66$  in this case.

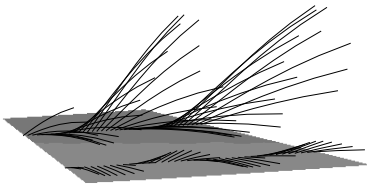


**Fig. 3.** Close-up of a part of Fig. 2.

In Fig. 2 we show a set of representative field lines having their foot points either close to the umbral-penumbral boundary or to the outer penumbral boundary. The field lines are chosen so that they outline locations of minimum and maximum inclination. The flutedness of the field is obvious. In Fig. 3 we show a slice of the full field over two wavelengths in azimuth to emphasize the details of the field structure a bit more. Especially in Fig. 3 we see that the field lines with the maximum inclination form long shallow loops across the penumbra as required for their association with the Evershed effect.

## 4. Discussion

### 4.1. Comparison with the linear force-free model

There are clear differences between this model and the linear force-free model of Martens et al. (1996). In the present model the field strength drops off with height more or less like  $1/z^2$

for large  $z$ . The variation of the inclination angle with height is completely determined by the function  $f$  we choose, but in any case it will have a much weaker dependence on  $z$  than the linear force-free model. In the linear force-free model, the magnetic field drops off exponentially and the scale height of the fluted part is very small. This is actually one of the shortcomings of that model.

Another difference is that the parts of the penumbra where the field is nearly horizontal do not form rather short loops but quite extended radial loops which can more easily account for the observed Evershed flow.

Whereas in the linear force-free model the direction and the amplitude of the current density are determined by the magnetic field because  $\alpha$  is a constant, in the present model  $\alpha^{(0)}$  is a function of the azimuth. The relation between  $\alpha^{(0)}$  and  $\gamma$  can be calculated either from Eq. (26) or Eq. (28). We get

$$\alpha^{(0)} = -\frac{1}{a} \frac{d\gamma}{d\phi} \quad (56)$$

With the form of  $\gamma$  given in Eq. (55), we obtain

$$\alpha^{(0)} = -\frac{m}{a} \bar{\delta}_{mod} \cos(m\phi) \quad (57)$$

Since the cosine has its extrema where the sine has its zeros and vice versa, we have the situation that the maximum current density flows along field lines having the average inclination, whereas the current density vanishes along field lines having the maximum or minimum inclination. Furthermore the direction of the current flow changes its sign every half wave length in azimuth. This coincides exactly with the discussion given

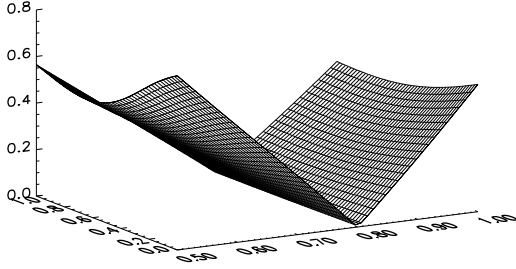


**Fig. 4.** Surface plot of the relative strength of the residual  $\mathbf{j} \times \mathbf{B}$ -force above the  $r$ - $z$ -plane for  $\phi = 0$ . The magnitude of the residual force stays well below 1, indicating that the quality of the approximation is reasonable.

in Title et al. (1993) and sketched in their Fig. 17. This vindicates our approach because it was our aim to come up with a self-consistent version of their schematic model.

#### 4.2. Quality of the approximation

An important point to investigate is the quality of the approximation scheme that we have presented. A good way to do this is to investigate the magnitude of the residual force due to the approximation. To be able to judge the quality of the approximation, we need to compare the residual force to a quantity of the same dimension. A convenient measure for the strength of the force is  $B^2(r, z)/\mu_0 L$ . We then obtain

$$\mu_0 L \frac{|\mathbf{j} \times \mathbf{B}|}{|\mathbf{B}|^2} = \frac{\mu_0 L |j_\phi|}{|\mathbf{B}|} = \frac{L \left| \frac{r}{a} - 1 \right| \frac{\partial B_z}{\partial \varpi}}{|\mathbf{B}|}. \quad (58)$$

Note that the residual force has only a poloidal component. One can immediately see that the residual force vanishes at the origin of the transformed coordinate system ( $r = a$ ). In Fig. 4 we show a surface plot of the residual force as function of  $r$  and  $z$  for  $\phi = 0$ . The plots for the locations of minimum and maximum inclination do not differ very much from this plot. It can be seen that the residual force is small close to the origin of the transformed radial coordinate system and then rises almost linearly in  $r$  away from that origin. This can be understood by an inspection of Eq. (58). Most of the variation of the residual force expression obviously comes from the factor  $|r/a - 1|$ . The factor  $\partial B_z / \partial \varpi / B$  just seems to be a minor modulation of the first factor. The plot also shows the limits of the approximation scheme. At the boundaries (in  $r$ ) the dimensionless residual force has reached a value of almost 0.6 which is at the very limit of what can be considered as acceptable for a small parameter. On the other hand, we have only considered the lowest order of the expansion scheme and higher order corrections could make the representation of the field even better. One should also keep in mind that by an expansion procedure like this one can usually not expect to get a convergent series but only an asymptotic series (though in a mathematically rig-

orous sense we would still need to prove that the series is indeed asymptotic).

We mention as a possibility that in principle, one could integrate the amplitude of the force over the volume under consideration and minimise this integral with respect to the parameter  $a$ . This would give a kind of optimum value for the location of the origin of the transformed  $r$ -coordinate. Since we expect that the increase in accuracy achieved by such a procedure will be small we have not carried this out here.

## 5. Conclusions

We have presented an expansion scheme that allows us to calculate self-consistent force-free solutions of the magnetohydrostatic equations with the basic properties of fluted sunspot penumbrae. The lowest order of the expansion produces equations which are mathematically equivalent to the equations describing laminated force-free solutions in Cartesian coordinates. The magnetic field then has no toroidal component in the lowest order and the magnetic field strength does not vary with azimuth. The field inclination, however, can have an arbitrary variation with azimuth. In comparison with the force-free model by Martens et al. (1996) the scale height of this variation is generally much larger.

We have calculated explicit solutions which have a profile of the magnetic field strength in the plane  $z = 0$  that exactly matches the profile given by Beckers & Schröter (1969). The field lines emerging from the plane  $z = 0$  extend across the penumbra in the radial direction and for the maximum inclination angle stay relatively shallow. This is consistent with the observations showing that the Evershed effect is basically associated with these field lines showing up as dark filaments in white light observations.

*Acknowledgements.* The authors thank Aad van Ballegooijen for useful discussions. TN acknowledges support by a PPARC Advanced Fellowship.

## References

- Beckers, J. M., Schröter, E. M. 1969, *Solar Phys.* 10, 384
- Degenhardt, D. & Wiehr, E. 1991, *A&A* 252, 821
- Kiessling, M. K.-H. 1995, *Statistical Mechanics of Weakly Dissipative Current-Carrying Plasma*, Habilitationsschrift, Ruhr-Universität Bochum, p. 29ff
- Low, B. C. 1988a, *ApJ* 330, 992
- Low, B. C. 1988b, *Sol. Phys.* 77, 43
- Lites, B. W., Scharmer, G. & Skumanich, A. 1990, *ApJ* 355, 329
- Martens, P. C. H., Hurlburt, N. E., Title, A. M., & Acton, L. W. 1996, *ApJ* 463, 372
- Neukirch, T. 1995, *A&A* 301, 628
- Neukirch, T. 1997, *A&A* 325, 847
- Shine, R. A., Title, A. M., Tarbell, T. D., Smith, K., Frank, Z. A. & Scharmer, G. 1994, *ApJ* 430, 413
- Rimmele, T. R. 1994, *A&A* 290, 972
- Rimmele, T. R. 1995a, *A&A* 298, 260
- Rimmele, T. R. 1995b, *ApJ* 445, 511
- Schatzman, E. 1965, in *Stellar and Solar Magnetic Fields*, IAU Symp. 22, ed. R. Lüft (New York: Wiley), 337

Stanchfield II, D. C. H., Thomas, J. H. & Lites, B. W. 1997, ApJ 477, 485

Title, A. M., Frank, Z. A., Shine, R. A., Tarbell, T. D., Topka, K. P., Scharmer, G., & Schmidt, W. 1993, ApJ 403, 780

Westendorp-Plaza, C., del Toro Iniesta, J. C., Ruiz Cobo, R., Martinez Pillet, V., Lites, B. W., Skumanich, A. 1997, Nature 389, 47